Journal of
Materials Chemistry B

Accepted Manuscript

This article can be cited before page numbers have been issued, to do this please use: M. C. Stefan, K. E. Washington, R. Kularatne, J. Du, Y. Ren, M. G. Gillings, C. Geng and M. C. Biewer, *J. Mater. Chem. B*, 2017, DOI: 10.1039/C7TB01291H.

ROYAL SOCIETY OF CHEMISTRY

rsc.li/materials-b

View Article Online
DOI: 10.1039/C7TB01291H

Journal of Materials Chemistry B

ARTICLE

Thermoresponsive star-like γ-substituted poly(caprolactone)s for micellar drug delivery

Received 00th January 20xx,
Accepted 00th January 20xx

DOI: 10.1039/x0xx00000x

www.rsc.org/

Katherine E. Washington, Ruvanthi N. Kularatne, Jia Du, Yixin Ren, Matthew J. Gillings, Calvin X. Geng, Michael C. Biewer, and Mihaela C. Stefan*

Temperature responsive drug carriers are attractive due to their ability to provide controlled release of the encapsulated cargo based on the use of external stimuli. In this work, 4- and 6-arm thermoresponsive star-like block copolymers were synthesized through the ring-opening polymerization of γ-substituted ε-caprolactone monomers γ-2-[2-(2-methoxyethoxy)ethoxy]ethoxy-ε-caprolactone (MEEECL) and γ-ethoxy-ε-caprolactone (ECL) using pentaerythritol and *myo*-inositol as multifunctional initiators. These amphiphilic block copolymers were shown to self-assemble into micelles and were characterized in terms of their feasibility as drug carriers. Both polymers were shown to be thermodynamically stable and demonstrated temperature responsivity in a desirable range for drug delivery, with lower critical solution temperatures of 39.4 °C and 39.8 °C for the 4- and 6-arm polymers, respectively. It was shown that the 6-arm star polymer had a higher drug loading capability and better stability *in vitro*, allowing it to function as a better vehicle for drug delivery in cytotoxicity experiments. These star polymers show promise as drug carriers due to their biocompatibility, biodegradability, and temperature controlled release of doxorubicin.

Introduction

Considerable efforts in recent years have aimed to develop smart drug carriers for improved delivery of anticancer drugs to tumor sites with increased efficiency and decreased side effects.[1-7] In particular, there is an interest in developing systems that can release their cargo in a triggered response either from the application of external stimuli or from a change in environment.[8-11] These systems allow for an increased control over where and when the encapsulated cargo is delivered and can be used to preferentially release drugs at tumor sites. Types of stimuli responsive polymers can include those that are sensitive to pH, temperature, reduction conditions, light, or multiple stimuli.

In the case of polymeric micellar drug delivery systems, polymers made from aliphatic polyesters such as poly(glycolide)s, poly(lactide)s, and poly(caprolactone)s have been studied extensively.[12, 13] Polyesters are attractive due to their biocompatibility and biodegradability through hydrolysis of esters in the backbone. Among these, poly(caprolactone)s are one of the most investigated materials due to the ease of property tunability through addition of substituents to the backbone.[14, 15] In this manner, substituents can affect the hydrophilicity or hydrophobicity of the polymer, provide stimuli responsiveness, and can play a role in micellar properties such as stability, size, degradation rate, and drug loading capabilities. The stability of these systems is of great importance. In order to function as drug carriers, it is imperative that they can stay intact upon dilution in the bloodstream.[16] In addition, the size can be used to passively target tumors through the enhanced permeability and retention (EPR) effect. Ideally, the particles should be in the size of 10-100 nm for this effect so that they are large enough to avoid clearance and small enough to bypass filtration in the spleen.[17-20] In these ways, polymeric micelles show promise for efficient delivery of poorly water soluble anticancer drugs while minimizing toxicity.

Temperature responsive polymers can be advantageous as polymeric micellar drug delivery systems, as they permit control over the release of the drug based on the application of localized heating or mild hyperthermia.[21] Polymers that display a lower critical solution temperature (LCST), provide a release mechanism of drug based on a solubility transition of the polymer in aqueous medium upon heating above the LCST. Previously, our group reported the synthesis of poly{γ-2-[2-(2-methoxyethoxy)ethoxy]ethoxy-ε-caprolactone} (PMEEECL) which was synthesized by *living* ring-opening polymerization of tri(ethylene glycol) substituted ε-caprolactone monomer.[22] This polymer has many advantages, including water solubility, and thermoresponsivity. Unlike other thermoresponsive polymers, PMEEECL is also biodegradable. When part of an amphiphilic block copolymer, it was shown that the LCST can be tuned depending on the hydrophobic block.[23-26] In addition, PMEEECL is an attractive candidate for the hydrophilic block on amphiphilic star polymers because it can be used in *living* ring-

Department of Chemistry and Biochemistry, The University of Texas at Dallas, Richardson, TX 75080, USA. *E-mail: mihaela@utdallas.edu; Fax: +1-972-883-2925; Tel: +1-972-883-6581

Electronic Supplementary Information (ESI) available: ^{1}H NMR spectra, SEC traces, TMAFM Height Images, degradation and absorbance curves for DOX loaded micelles.

See DOI: 10.1039/x0xx00000x

opening polymerization which allows tunability of the system through control over the molecular weight and composition.

In an effort to expand on previously reported linear polymers featuring PMEEECL, 4- and 6- arm star-like block copolymers containing PMEEECL as the hydrophilic block and poly(γ-ethoxy-ε-caprolactone) (PECL) as the hydrophobic block were synthesized. These systems were examined to determine the effects of the architecture on the thermoresponsivity, stability, and drug loading. Star-like polymers have an increased density of functional units compared to linear polymers, and have been shown to have many promising attributes for drug delivery, including increased drug loading.[27, 28] Herein, we report the first thermoresponsive star polymers synthesized using PMEEECL, and compare the resulting properties with their previously reported linear counterpart.

Results and Discussion

Polymer Synthesis

In a previous report from our group, a linear block copolymer consisting of ECL and MEEECL was examined for its thermoresponsivity, thermodynamic stability, and drug loading capabilities.[24] The linear block copolymer was synthesized through *living* ring-opening polymerization of γ-ethoxy-ε-caprolactone (ECL) and γ-2-[2-(2-methoxyethoxy)ethoxy] ethoxy-ε-caprolactone (MEEECL) monomers using stannous (II) 2-ethylhexanoate ($Sn(Oct)_2$) as the catalyst and benzyl alcohol as the initiator. This polymer showed promise in terms of temperature responsivity and thermodynamic stability, however it was shown to have limited drug loading capacity (2.05 wt. %). In an attempt to increase the drug loading and the stability, two functionalized star-like diblock polycaprolactones were synthesized. The ECL and MEEECL monomers were synthesized according to previous published procedures (Scheme 1) and were used for the hydrophobic and hydrophilic block respectively.[22, 24] The star polymers were synthesized with $Sn(Oct)_2$ as the catalyst and two different multifunctional alcohol initiators were employed to form the 4-arm (pentaerythritol initiator) and 6-arm (*myo*-inositol initiator) block copolymers (Scheme 2). The polymerizations were carried out at 110 °C with sequential monomer addition, starting with the polymerization of the hydrophobic ECL monomer. The polymerizations used the following molar ratios to target a

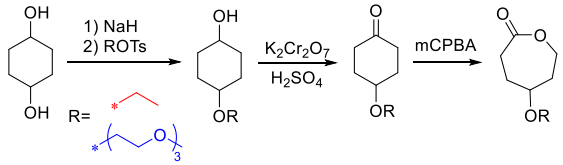

Scheme 1. Synthesis of γ-2-ethoxy-ε-caprolactone and γ-2-[2-(2-methoxyethoxy)ethoxy]ethoxy-ε-caprolactone, functionalized ε-caprolactone monomers

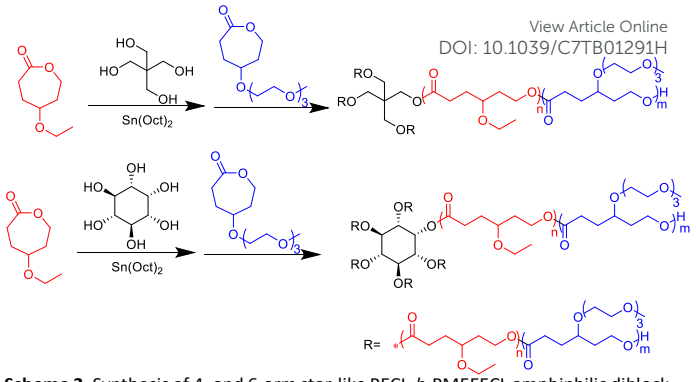

Scheme 2. Synthesis of 4- and 6-arm star-like PECL-*b*-PMEEECL amphiphilic diblock copolymers

Table 1. Summary of polymer compositions and molecular weight

	M_n (g mol^{-1})[a]	PDI[a]	mol % ECL[b]	mol % MEEECL[b]
4A	20,400	1.1	49.7	50.3
6A	28,800	1.4	47.2	52.8

[a]Determined by size exclusion chromatography with THF as eluent [b]Determined by ^{1}H NMR Spectroscopy

50:50 molar composition of hydrophilic to hydrophobic block: [Initiator]: [$Sn(Oct)_2$]: [ECL]: [MEEECL], [1]: [4]: [50]: [50] for the 4-arm polymer (**4A**) and [1]: [6]: [50]: [50] for the 6-arm polymer (**6A**). This composition was targeted in an effort to generate comparable composition and molecular weights to the previously published linear block copolymer.[24] The ^{1}H NMR spectra are shown in Figures S1 and S2, and a summary of the molecular weights and composition of the polymers is shown in Table 1. The compositions were determined by the integration of the peaks of the substituents of the block copolymers, the methoxy group on the oligo ethylene glycol substituent at ~3.37 ppm was integrated versus the methyl group of the ethoxy substituent at ~1.17 ppm. The molecular weights of the two polymers were determined by size exclusion chromatography (SEC) equipped with a triple detection system, allowing for the determination of the absolute molecular weight. Additional information from SEC measurements, including the SEC traces and hydrodynamic radius, can be found in the supporting material (Figures S3 and S4 and Table S1). The polymers were shown to have comparable compositions to each other as well as the linear polymer, with **6A** having a slightly higher molecular weight and both polymers having fairly narrow PDI.

Self-Assembly and Thermoresponsivity

The lower critical solution temperature (LCST) of the polymers was determined by measuring the change in transmittance with increasing temperature. Transmittance decreases above the LCST due to the dehydration and precipitation of the polymer from the aqueous solution. The transmittance was measured with a UV-vis spectrophotometer at 600 nm. The LCST was taken as the temperature where there is a 50% drop in the transmittance during heating (Figure 1 A

View Article Online
DOI: 10.1039/C7TB01291H

Table 2. Summary of polymeric micelle properties

	CMC ($g\ L^{-1}$)[a]	LCST (°C)[b]	D_h (nm)[c]	Size Dispersity[c]
4A	1.68×10^{-3}	39.8	80.85	0.085
6A	1.37×10^{-3}	39.4	50.98	0.131

[a]Determined by fluorescence spectroscopy with pyrene as a fluorescent probe [b]Measured with UV-vis as the 50% drop in transmittance at 600 nm upon heating aqueous polymer solution [c] Hydrodynamic diameter of micelles at 25 °C determined from dynamic light scattering

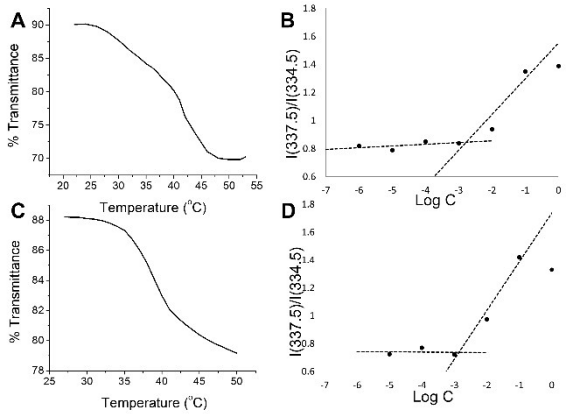

Fig. 1 Transmittance and CMC plots showing thermoresponsiveness and thermodynamic stability of **4A** (A and B) and **6A** (C and D) respectively.

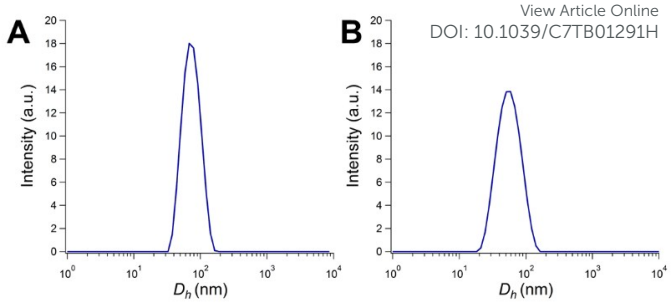

Fig. 2 Size distribution (D_h) for **4A** (A) and **6A** (B) polymeric micelles at 25 °C obtained from DLS.

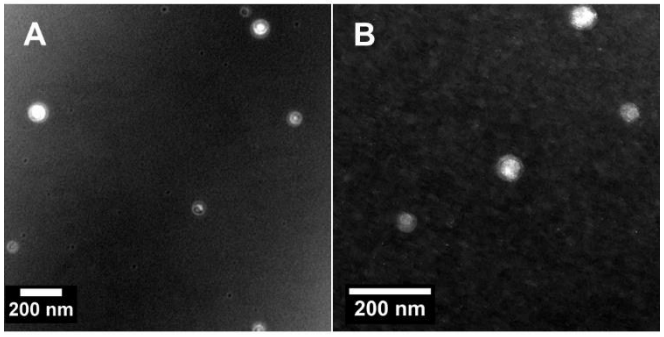

Fig. 3 TEM images of empty micelles (A) **4A** and (B) **6A**.

and C). The LCST of **4A** and **6A** were comparable, with **4A** showing LCST of 39.4 °C and **6A** with LCST of 39.8 °C (Table 2). These LCST values are useful for drug delivery applications since they are higher than physiological temperature (37 °C), meaning the micelles will be stable as they circulate in the bloodstream, and below 40 °C allowing the application of external temperature to release the encapsulated cargo. Importantly, these polymers show improved LCST values over the previously reported linear polymer, which had an LCST below physiological temperature.

The critical micelle concentration (CMC) was determined by fluorescence spectroscopy using pyrene as a probe.[29] The pyrene excitation spectrum shows a peak shift from 334.5 nm to 337.5 nm as pyrene goes from a hydrophilic environment into the hydrophobic core of the micelle. The intensity ratio ($I_{337.5}/I_{334.5}$) was plotted against the logarithm of the polymer concentration, where the intersection of the two slopes is estimated as the CMC (Figure 1, B and D). The estimated CMC value for **4A** is 1.68×10^{-3} g L^{-1} and for **6A** is 1.37×10^{-3} g L^{-1} (Table 2). The CMCs for these polymers are fairly similar, however in comparison with the previously synthesized linear block copolymers (8.95×10^{-3} g L^{-1}), the values are almost a magnitude lower indicating that the star polymers have better thermodynamic stability.[24] This could be due to the increased density of the functional groups in the star polymer allowing increased hydrophobic interactions.

Size and Morphology

The size and morphology of the empty polymeric micelles were investigated by dynamic light scattering (DLS) and transmission electron microscopy (TEM). Empty micelles were prepared by dialysis method at a concentration of 1 mg mL^{-1}. The micelles were examined with dynamic light scattering (DLS) to determine the hydrodynamic diameter (D_h) and the dispersity of the sample. The micelles exhibited sizes of 80.85 nm and 50.98 nm for **4A** and **6A,** respectively (Table 2, Figure 2). The micelles formed from polymer **6A** were much smaller in size when compared to those formed from **4A**. In order to observe the morphology, TEM was performed using phosphotungstic acid for negative staining. Amphiphilic block copolymers can assemble into various structures such as spherical micelles, vesicles, or cylindrical micelles depending on several factors including the composition of the block copolymer, the molecular weight, the solvent system, or environment. [30] The star block copolymers formed spherical micelles in aqueous solution which was visualized from the TEM images (Figure 3). This was expected based on our previous results with star polymers formed from substituted polycaprolactones with PMEEECL as the hydrophilic block.[31] The sizes measured from TEM were comparable to the values obtained with DLS. However, unlike the distribution observed with DLS, there appeared to be more variation in size observed in the TEM images.

Doxorubicin Encapsulation

To determine the feasibility of using the star block copolymers as drug carriers, doxorubicin (DOX) was loaded into the micelles through dialysis method. The absorbance of the DOX loaded micelles measured at 485 nm was fitted against a pre-established calibration curve in order to determine the concentration of the loaded drug. (Figure S5) The drug loading

content (DLC) and encapsulation efficiency (EE) were determined using the following equations:

$$DLC = \frac{weight\ of\ encapsulated\ DOX}{weight\ of\ polymer}\ x\ 100$$

$$EE = \frac{weight\ of\ encapsulated\ DOX}{weight\ of\ total\ DOX}\ x\ 100$$

We speculated that the 6-arm polymer (**6A**) would have a higher drug loading than the 4-arm polymer (**4A**) due to increased density of functional units in the core of the micelle. Moreover, based on previous data which showed that star polymers have increased loading over linear polymers, we predicted that both of the star polymers would have a higher loading than the previously synthesized linear block copolymers (2.05 wt.%).[24, 31] The DOX loading was performed in the same conditions as the earlier published linear block copolymers, and at the same ratio (10:1 polymer: drug) to allow comparison of the loading. Polymer **4A** was shown to have a DLC of 2.06 wt.%, while polymer **6A** had a DLC of 2.63 wt.%. Polymer **4A** had a drug loading comparable to that of the reported value of the linear block copolymer, while polymer **6A** had the highest DLC and encapsulation efficiency. The increased loading could be due to the increased density of functional groups in the core provided by the 6-arms. It is worth noting that **6A** had a higher molecular weight than **4A** which could influence the loading as well. A summary of the drug loading is shown in Table 3. The change in size and the morphology was investigated after loading DLS, tapping mode atomic force microscopy (TMAFM), and TEM. The micelles retained their spherical shape after loading and both star block copolymers showed an increase in size after loading (Fig 4). As observed before, the sizes measured from TEM showed good correlation with those measured from DLS. Even after loading, the micelles retained a size ideal for passive targeting using the EPR effect, with **4A** having the largest size, at 102.8 nm. (Fig 5)

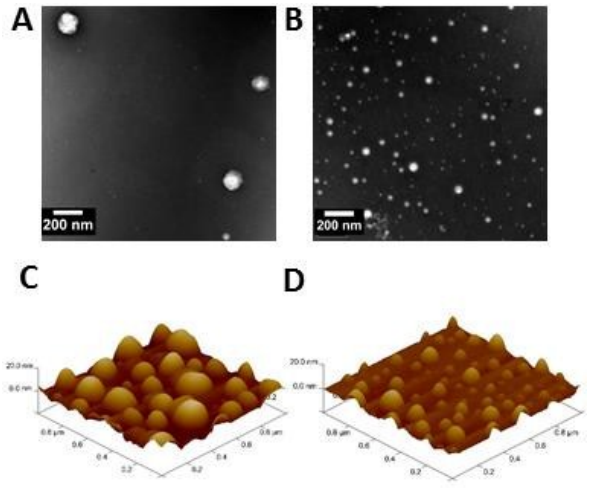

Fig. 4 TEM images of DOX loaded micelles (A) **4A** and (B) **6A**, scale bar = 200 nm. TMAFM images of DOX loaded polymeric micelles (C) **4A** and (D) **6A** deposited on mica substrate, scan size:1 µm

Table 3. Summary of DOX loaded polymeric micelles

	DLC (wt. %)[a]	EE (wt. %)[a]	D_h^{DOX} (nm)[b]	Size Dispersity[b]
4A	2.06	20.6	102.8	0.155
6A	2.63	26.3	64.5	0.159

[a]Determined with UV-Vis spectroscopy, absorbance measured at 485 nm
[b]Determined through dynamic light scattering at 25 °C

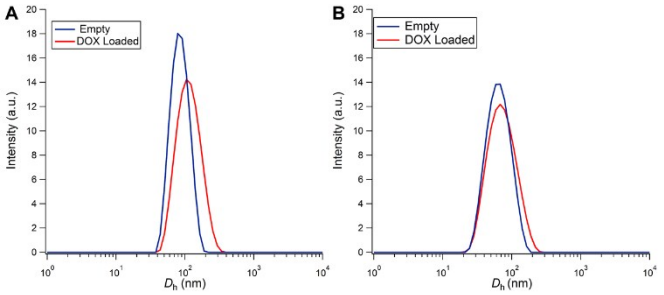

Fig. 5 Size distribution obtained through DLS for (A) **4A** and (B) **6A** comparing the sizes of empty and DOX loaded micelles

Biocompatibility and Degradation

The biodegradability of the star block copolymer **6A** was examined by dissolving the polymer in PBS (pH =7.4) and stirring the solution at 37 °C for several days. The degradation was measured by determining the % change in molecular weight over time (Figure S7). The polymer showed degradation over several days indicating the polymer was biodegradable in physiological conditions. It can be assumed that polymer **4A** would be degradable over time as well since it has similar structure and composition. It has been shown recently that although star-like polyesters degrade at a slower rate than linear polymers, the number of arms does not affect the rate of degradation as significantly.[32]

To evaluate the biocompatibility of these polymers, cytotoxicity measurements were performed using various concentrations of the empty polymers on HeLa cells. CellTiter-Blue® cytotoxicity kit was used to examine the cell viability after the cells had been exposed to the polymer solutions for 24 hours. The polymers were not shown to exhibit significant toxicity to the cells even up to 0.5 mg mL^{-1} (Fig 6). According to these measurements, the polymers display excellent biocompatibility as well as biodegradability under physiological conditions.

***In Vitro* Drug Release of Doxorubicin**

The *in vitro* release was determined for **4A** and **6A** at physiological temperature (37 °C) and above their LCST (40 °C) in PBS buffer (pH 7.4) and is shown in Fig. 7. Although DOX was released at both temperatures, the initial release rate was higher for the micelles incubated at 40 °C and the overall release was the highest for the micelles incubated at the higher temperature, with the cumulative release reaching around 60% after 48 hours. This indicates that there is some thermal control over the release of DOX, especially within the first 24 hours.

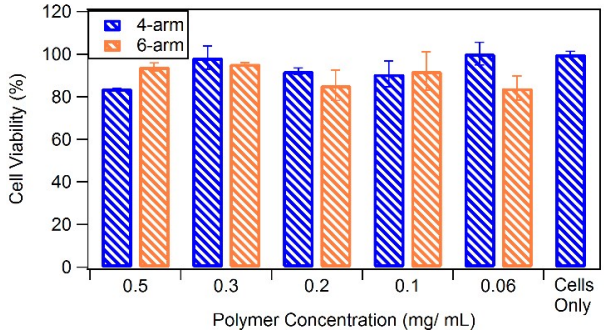

Fig. 6 Cell viability measurements of varying concentrations of empty polymeric micelles in PBS using HeLa cells and CellTiter-Blue ® to measure cell viability, n=4.

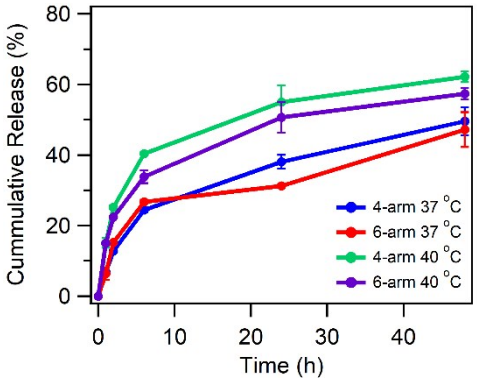

Fig. 7 Release profiles of DOX from 4A and 6A above (40 °C) and below (37 °C) their LCSTs in PBS buffer solution (pH 7.4), n=3.

Stability of Micelles in FBS

The stability of micelles *in vivo* can be greatly influenced by serum proteins. To investigate the potential use of the star polymer micelles as drug carriers *in vivo*, their stability over time in PBS and PBS supplemented with 10% FBS (which is similar to the concentration in blood plasma) was examined (Fig 8). The micelles were prepared by loading**4A** and **6A** with Nile Red (NR) and the fluorescence was monitored over time. NR is a molecule that strongly fluoresces in hydrophobic

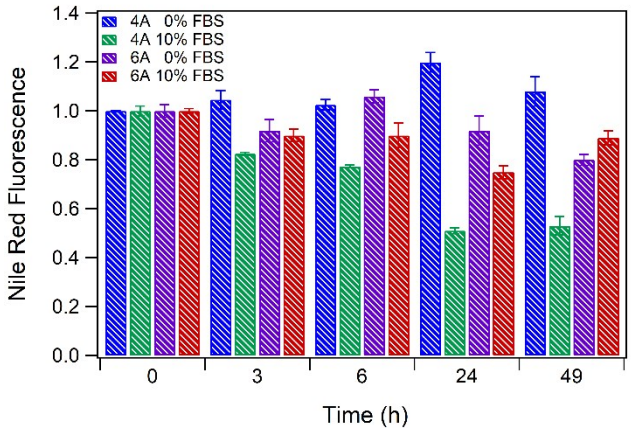

Fig. 8 Stability of Nile Red loaded micelles over time in PBS containing either 0% or 10% FBS, n=3.

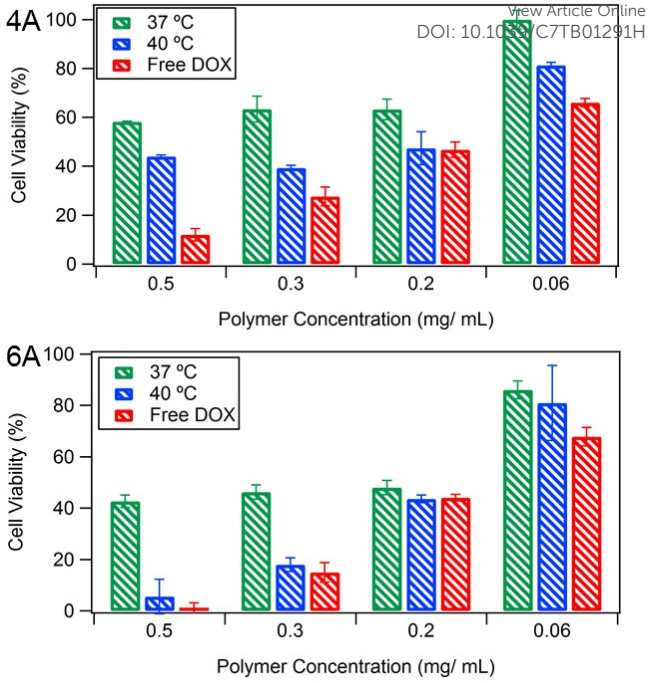

Fig. 9 Cell viability of HeLa cells after dosing with DOX loaded micelles above and below the LCST

environments such as the core of a micelle, and the emission intensity decreases as it is exposed to aqueous environment. For the micelles incubated in PBS only, there was no significant change in fluorescence observed for the micelle solutions over 48 hours. In the case of the micelles incubated in PBS containing FBS, there was a visible change in NR loaded **4A** after 24 hours, indicating that there could be drug released after exposure to serum proteins. However, there was only a slight decrease in the fluorescence of NR loaded **6A** indicating more stability over time.

Cytotoxicity and Cellular Uptake of DOX Loaded Micelles

The cytotoxicity of the DOX loaded micelles was examined using HeLa cells at various concentrations. In the interest of determining the temperature controlled release of DOX in cells, the cells were incubated at either physiological temperature (37 °C) or at a temperature above the LCST of the polymers (40 °C). HeLa cells were dosed with DOX loaded micelles and allowed to incubate at either temperature for 24 hours. The cell viability was measured using CellTiter-Blue® assay. It was observed at all concentrations that the release of DOX was more substantial at temperatures above the LCST causing less cells to be viable. Free DOX was administered to HeLa cells as well in concentrations coinciding with the amount loaded into the star polymer micelles based on the DLC determined. In all cases, the free DOX showed higher cytotoxicity to the cells, however the cells exposed to DOX loaded micelles at temperatures higher than the LCST exhibited cytotoxicity closer to that of the free DOX dosages (Fig 8), which correlates with what was observed in the *in vitro* release (Fig 7). The DOX loaded **6A** micelles exhibited higher toxicity than the DOX loaded **4A** micelles,

View Article Online
DOI: 10.1039/C7TB01201H

which can be attributed to the higher loading capabilities of the **6A** micelles.

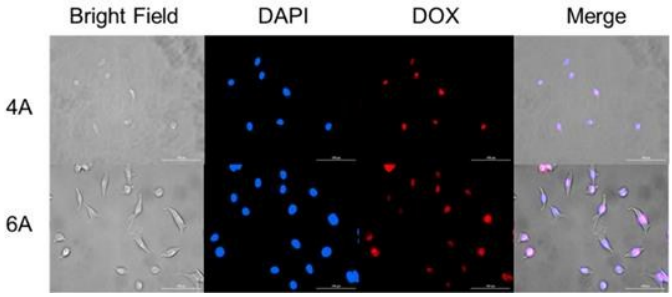

Fig 10. Uptake of **4A** and **6A** DOX loaded micelles in HeLa cells after incubating for 4 hours. Cell nuclei were stained with DAPI.

The ability of the micelles to be taken into the cancer cell was observed through cellular uptake experiments using HeLa cells. The DOX loaded micelles were added to HeLa cells and incubated for 4 hours. At that time, the cells were washed and the nuclei were counterstained with DAPI to visualize the cell nuclei through fluorescence microscopy, shown in Fig 10. The red signal, attributed to DOX can be seen within the cell nuclei, indicating the endocytosis of the micelles into the cell and the internalization of DOX into the nucleus of the cell.

Experimental

Materials

All commercially available chemicals were purchased from Sigma Aldrich or Fisher Scientific and used without further purification unless otherwise noted. Benzyl alcohol and $Sn(Oct)_2$ were purified through vacuum distillation prior to use. All polymerization reactions were conducted under purified nitrogen in glassware that was dried at 120 °C for at least 24 hours and cooled in a desiccator prior to use.

Analysis

^{1}H NMR spectra of the synthesized monomers and polymers were recorded on a Bruker AVANCE III 500 MHz NMR instrument at 25 °C in $CDCl_3$. ^{1}H NMR data are reported in parts per million as chemical shifts relative to tetramethylsilane (TMS) as the internal standard. GC/MS was performed on an Agilent 6890-5973 GC/MS workstation. Molecular weight and polydispersity indices of the synthesized polymers were measured by SEC analysis on an OMNISEC multi-detector system equipped with Viscotek columns (T6000M), connected to a refractive index (RI), low angle light scattering (LALS), right angle light scattering (RALS), and viscosity detectors with HPLC grade THF as the eluent, and triple point calibration based on polystyrene standards. Fluorescence spectra of the synthesized polymers were collected with a Perkin-Elmer LS 50 BL luminescence spectrometer at 25 °C with emission wavelength set at 390 nm. LCST measurements were performed using a temperature controlled Cary5000 UV-Vis spectrometer. DLS measurements were performed using a Malvern Zetasizer Nano ZS instrument equipped with a He–Ne laser (633 nm) and 173° backscatter detector. TEM imaging of the DOX-loaded micelles was performed on a Tecnai G2 Spirit Biotwin microscope by FEI and images were analyzed using Image J software. Samples were prepared by treating copper mesh grid with 1 mg mL^{-1} aqueous polymer micelle solution for 2 minutes, followed by staining with 2% phosphotungstic acid for 30 seconds. TMAFM images were obtained by depositing the DOX loaded micelles on freshly cleaved mica substrate and allowing to air dry and using a VEECO-dimension 5000 Scanning Probe Microscope with silicon cantilever with spring constant 42 nm^{-1}. Images were acquired at 1 Hz scan frequency and analysed with Nanoscope 7.30 software to generate the 3D renderings. Absorbance spectra for DOX loading determination was recorded using an Agilent UV/Vis spectrophotometer. Cytotoxicity and cellular uptake measurements were performed with a Biotek Cytation 3 imaging reader.

Synthetic Procedures

The synthesis of monomers MEEECL and ECL were performed according to previously published procedures and are shown in Scheme 1.[24]

Synthesis of 4-arm star-like PMEECL-*b*-PECL. ECL (0.387 g, 0.00245 mol) was added into a Schlenk flask and stirred under vacuum for one hour. At that time, pentaerythritol (4.17 mg, 3.1 x 10^{-5} mol) and $Sn(Oct)_2$ (53 mg, 1.2 x 10^{-5} mol) were added in 0.3 mL toluene under a nitrogen atmosphere to the reaction flask. The reaction was introduced into a thermostatted oil bath at 110 °C. The consumption of monomer was monitored using GC/MS. After ECL was consumed, previously dried MEEECL (0.7 g, 0.00245 mol) was added in 0.2 mL of toluene to the reaction flask under nitrogen. The polymerization was allowed to continue over night and after the MEEECL was consumed, the reaction was quenched by precipitation in hexane, yielding 0.8 g of clear gel-like polymer.
^{1}H NMR (500 MHz, $CDCl_3$, δ): 1.163 (t, 3H), 1.772 (m, 6H), 1.856 (m, 3H), 2.380 (t, 4H), 3.373 (s, 3H), 3.469 (m, 4H), 3.546 (m, 2H), 3.597 (m, 4H), 3.644 (m, 7H), 4.161 (m, 4H)

Synthesis of 6-arm star-like PMEEECL-*b*-PECL. ECL (0.224 g, 0.0014 mol) was added into a Schlenk flask and stirred under vacuum for one hour. At that time, *myo*-inositol (3.2 mg, 1.8 x 10^{-5} mol) and $Sn(Oct)_2$ (45 mg, 1.1 x 10^{-5} mol) were added in 0.3 mL toluene under a nitrogen atmosphere to the reaction flask. The reaction was introduced into a thermostatted oil bath at 110 °C. The consumption of monomer was monitored using GC/MS. After ECL was consumed, previously dried MEEECL (0.4 g, 0.0014 mol) was added in 0.2 mL of toluene to the reaction flask under nitrogen. The polymerization was allowed to continue over night and after the MEEECL was consumed, the reaction was quenched by precipitation in hexane, yielding 0.5 g of clear gel-like polymer.
^{1}H NMR (500 MHz, $CDCl_3$, δ): 1.165 (t, 3H), 1.785 (m, 6H), 1.857 (m, 3H), 2.382 (t, 4H), 3.375 (s, 3H), 3.471 (m, 4H), 3.547 (m, 2H), 3.599 (m, 4H), 3.646 (m, 7H), 4.1632 (m, 4H)

View Article Online
DOI: 10.1039/C7TB01291H

Determination of LCST

To determine the LCST, 2 mg of polymer was dissolved in 10 mL of water to make a 0.2 wt. % solution. The % transmittance at 600 nm was recorded at temperatures ranging from 25 °C to 55 °C. The LCST or cloud point was taken at the point of 50% drop in transmittance for each sample.

Preparation of Micelles

Polymeric micelles were formed through nanoprecipitation and dialysis. The polymer (5 mg) was dissolved in THF (0.4 mL) and added dropwise to 5 mL of water under sonication. The resulting micelle suspension was transferred to SnakeSkin® dialysis tubing (MWCO 3500 Da) and dialyzed against a minimum of 1500 mL deionized water over a 24-hour period. The final contents of the dialysis tubing were filtered through a Nylon syringe filter (0.22 µm) to obtain a polymeric micelle solution with a concentration of 1 mg mL^{-1}.

Preparation of DOX Loaded Micelles

DOX-loaded micelles were prepared in a manner similar to the empty micelles. DOX·HCl was first neutralized by adding 3 equivalents of triethylamine in DMSO. An aliquot of the neutralized DOX solution containing 0.5 mg of DOX was added to a polymer solution (5 mg in 0.4 mL DMSO). The DOX-polymer solution was then added dropwise into 5 mL of deionized water under sonication. The resulting suspension was transferred to dialysis tubing and dialyzed against a minimum of 1500 mL of deionized water over a 24 hour period. The contents of the dialysis tube were finally filtered using a Nylon syringe filter (0.45 µm) to obtain a 1 mg mL^{-1} solution of DOX loaded micelles. To determine the DLC and EE, the drug loaded micelle solutions were diluted with DMSO in a 1:1 ratio to break the micelles. The absorbance of the solution at 485 nm was fitted to a pre-established standard curve of DOX in DMSO/ DI H_2O.

Determination of CMC

The CMC was determined using pyrene, a hydrophobic fluorescent molecule, as a probe. Various concentrations of polymer samples were combined with a small amount of pyrene (6.0×10^{-5} M in THF) in 0.2 mL THF. The polymer/pyrene samples were added dropwise into 10 mL of deionized water. The resulting solutions were stirred for 4h to allow micelle assembly and complete evaporation of THF. The resulting solutions contained concentrations from 1×10^{-5} to 1 g L^{-1} of polymer and a constant concentration of pyrene. Fluorescence spectra of the polymer/pyrene solutions were collected at 25 °C with emission wavelength of 390 nm. The ratio of intensities of the pyrene excitation peaks at 337.5 nm and 334.5 nm were recorded and plotted against the logarithm of the polymer concentration (C). The x coordinate at the intersection of the two trend lines before and after the abrupt increase in the $I_{337.5}/I_{334.5}$ vs. Log (C) curve was taken to be the critical micelle concentration.

DLS Analysis

Aqueous suspensions of micelles were prepared as stated above at a concentration above the determined CMC, at 1 mg mL^{-1}. The micelles were analyzed to determine their hydrodynamic diameters (D_h) using dynamic light scattering. Prior to measurement, the polymer micelle solutions were filtered with a 0.22 µm nylon syringe filter. Size measurements were recorded at 25 °C in triplicate.

Demonstration of Polymer Degradation

A sample of polymer (15 mg) was dissolved in 3 mL of PBS (pH 7.4, DNase-, RNase-, and Protease-Free) and was stirred in a closed system in a thermostatted oil bath at 37 °C over a period of 6 days. Samples were taken periodically and analyzed by SEC to monitor the change in M_n from t=0 to t=6 days. The resulting change in molecular weight is plotted as % of initial M_n vs. days spent in PBS solution at 37 °C.

Biological Studies

Unless otherwise indicated, all cell culture experiments were performed using RPMI-1640 medium with L-glutamine and sodium bicarbonate supplemented with 10% fetal bovine serum and 1% penicillin-streptomycin. Cells were grown in a humidified environment at 37 °C, 5% CO_2. Cell viability studies were performed using the CellTiter-Blue® assay (Promega) according to the manufacturer's recommended protocol.

***In vitro* DOX Release**

A 1 mg mL^{-1} solution of DOX loaded micelles were prepared as previously described. DOX loaded solution (2 mL) was transferred to dialysis membrane tubes with MWCO of 3500 Da. The tubes were immersed in beakers of pH 7.4 PBS solutions (10 mL) and stirred at a constant speed at either 37 °C or 40 °C. At specific time intervals, 2 mL of the release medium was withdrawn and replaced with fresh solution. The DOX content in the samples was analysed using UV-Vis spectroscopy. Absorbance measurements in the release media were taken at 485 nm to calculate the cumulative DOX release.

Stability of Micelles in FBS

NR loaded micelles were prepared in the same method as DOX loaded micelles and were incubated in PBS containing either 0% or 10% FBS. The fluorescence emission intensity was measured at 632 nm at desired time points. The NR emission intensities are normalized to the initial fluorescence intensities (t=0) and plotted versus time.

Empty Micelle Cytotoxicity Studies

HeLa cells were seeded in transparent flat-bottom 96-well plates at a cell density of 5,000 cells per well in 100 µL growth medium. After 24h to allow cell adhesion, the medium was removed, the cells were washed with 100 µL PBS, and 100 µL fresh growth medium was added to each well. Empty micelles (1 mg mL^{-1} in PBS) were diluted to concentrations ranging from 0.06 mg mL^{-1} to 0.5 mg mL^{-1}. Micelle dilutions (100 µL) were

added to the cells via multichannel micropipette. The micelles were incubated for 24 hours with the cells. At this time, the cell viability was evaluated by the CellTiter-Blue® assay, N=4.

DOX-loaded Micelle Cytotoxicity Studies

HeLa cells were seeded in transparent flat-bottom 96-well plates at a cell density of 5,000 cells per well in 100 µL growth medium. After 24h to allow cell adhesion, the medium was removed, the cells were washed with 100 µL PBS, and 100 µL of fresh growth medium was added to the cells. DOX-loaded micelles (1 mg mL^{-1} in PBS) were diluted in PBS to concentrations ranging from 0.06 mg mL^{-1} to 0.5 mg mL^{-1}. DOX-loaded micelle dilutions (100 µL) were added to the cells via multichannel micropipette. Free DOX dosing was given assuming the dose from the predetermined drug loading. The cells were then incubated at either 37 °C or 40 °C for 24 hours with the DOX-loaded micelles. After this time, the cell viability was evaluated using the CellTiter-Blue® assay, N=4.

Cellular Uptake

HeLa cells were seeded in a 35-mm glass bottom dish at a density of 200,000 cells per well and allowed to adhere for 24 h in 2 mL of growth media. At that time, the medium was removed, the cells were washed with 2mL of PBS, and 2 mL of fresh growth medium was added along with 1 mL of DOX-loaded micelles (0.2 mg mL^{-1} in PBS). The cells dosed with DOX-loaded micelles were allowed to incubate for 4 hours. After the uptake period, the cells were washed 3 times with 2 mL of PBS, fixed with 4% paraformaldehyde (room temperature, 10 minutes), washed 3 times with 2 mL of PBS, and the nuclei were counterstained with DAPI. Images were obtained using a BioTek Cytation 3 Cell Imaging Multi-Mode Reader.

Conclusions

Temperature responsive 4- and 6-arm amphiphilic star-like polycaprolactones were successfully synthesized through the *living* ring-opening polymerization of functionalized ε-caprolactone monomers ECL and MEEECL. The use of the MEEECL monomer enables the synthesis of star-like polymers through with high control over the composition and molecular weight, while also allowing the resulting polymers to be thermoresponsive. These polymers were thermodynamically stable with CMCs ~10^{-3} g L^{-1}. Additionally, the star block copolymers had LCST above the physiological temperature of 37°C which is desirable for use in temperature controlled drug delivery. These polymers were also shown to be biocompatible, exhibiting relatively low toxicity to HeLa cells at doses up to 0.5 mg mL^{-1}, and biodegradable over time under physiological conditions. Drug release studies showed that the release of drug increased with the application of external temperature in both micellar system and cytotoxicity studies indicated increased toxicity to cancer cells when incubated at temperatures higher than LCST, indicating that these systems show thermally controlled release. These drug delivery systems showed improvement over the previously reported linear polymer in terms of their thermodynamic stability as well as their LCSTs. Future optimization of these drug delivery systems will focus on improving the drug loading capabilities either through changes in the substituents of the hydrophobic block or through different loading methods.

Acknowledgements

We gratefully acknowledge the financial support from National Science Foundation (CHE-1609880) and Welch Foundation (AT-1740).

Notes and references

1. K. Kataoka, A. Harada and Y. Nagasaki, *Advanced Drug Delivery Reviews*, 2001, **47**, 113-131.
2. Z. Ahmad, A. Shah, M. Siddiq and H.-B. Kraatz, *RSC Advances*, 2014, **4**, 17028-17038.
3. S. Biswas, P. Kumari, P. M. Lakhani and B. Ghosh, *European Journal of Pharmaceutical Sciences*, 2016, **83**, 184-202.
4. S. Movassaghian, O. M. Merkel and V. P. Torchilin, *Wiley Interdisciplinary Reviews: Nanomedicine and Nanobiotechnology*, 2015, **7**, 691-707.
5. A. Rösler, G. W. M. Vandermeulen and H.-A. Klok, *Advanced Drug Delivery Reviews*, 2012, **64, Supplement**, 270-279.
6. T. M. Allen and P. R. Cullis, *Science*, 2004, **303**, 1818.
7. A. Rahikkala, V. Aseyev, H. Tenhu, E. I. Kauppinen and J. Raula, *Biomacromolecules*, 2015, **16**, 2750-2756.
8. D. Schmaljohann, *Advanced Drug Delivery Reviews*, 2006, **58**, 1655-1670.
9. S. Mura, J. Nicolas and P. Couvreur, *Nat Mater*, 2013, **12**, 991-1003.
10. M. A. C. Stuart, W. T. S. Huck, J. Genzer, M. Muller, C. Ober, M. Stamm, G. B. Sukhorukov, I. Szleifer, V. V. Tsukruk, M. Urban, F. Winnik, S. Zauscher, I. Luzinov and S. Minko, *Nat Mater*, 2010, **9**, 101-113.
11. V. P. Torchilin, *Nat Rev Drug Discov*, 2014, **13**, 813-827.
12. K. E. Washington, R. N. Kularatne, V. Karmegam, M. C. Biewer and M. C. Stefan, *Wiley Interdisciplinary Reviews: Nanomedicine and Nanobiotechnology*, 2016, DOI: 10.1002/wnan.1446, DOI.
13. O. Coulembier, P. Degée, J. L. Hedrick and P. Dubois, *Progress in Polymer Science*, 2006, **31**, 723-747.
14. E. A. Rainbolt, K. E. Washington, M. C. Biewer and M. C. Stefan, *Polymer Chemistry*, 2015, **6**, 2369-2381.
15. H. Jing, A. R. Elizabeth, W. Katherine, C. B. Michael and C. S. Mihaela, *Current Organic Chemistry*, 2013, **17**, 930-942.
16. M. L. Adams, A. Lavasanifar and G. S. Kwon, *Journal of Pharmaceutical Sciences*, 2003, **92**, 1343-1355.
17. H. Maeda, H. Nakamura and J. Fang, *Advanced Drug Delivery Reviews*, 2013, **65**, 71-79.
18. J. Wang, W. Mao, L. L. Lock, J. Tang, M. Sui, W. Sun, H. Cui, D. Xu and Y. Shen, *ACS Nano*, 2015, **9**, 7195-7206.
19. H. Maeda, *Advanced Drug Delivery Reviews*, 2015, **91**, 3-6.
20. Z. L. Tyrrell, Y. Shen and M. Radosz, *Progress in Polymer Science*, 2010, **35**, 1128-1143.
21. D. Roy, W. L. A. Brooks and B. S. Sumerlin, *Chemical Society Reviews*, 2013, **42**, 7214-7243.
22. J. Hao, J. Servello, P. Sista, M. C. Biewer and M. C. Stefan, *Journal of Materials Chemistry*, 2011, **21**, 10623-10628.

View Article Online
DOI: 10.1039/C7TB01291H

23. Y. Cheng, J. Hao, L. A. Lee, M. C. Biewer, Q. Wang and M. C. Stefan, *Biomacromolecules*, 2012, **13**, 2163-2173.
24. J. Hao, Y. Cheng, R. J. K. U. Ranatunga, S. Senevirathne, M. C. Biewer, S. O. Nielsen, Q. Wang and M. C. Stefan, *Macromolecules*, 2013, **46**, 4829-4838.
25. E. A. Rainbolt, J. B. Miller, K. E. Washington, S. A. Senevirathne, M. C. Biewer, D. J. Siegwart and M. C. Stefan, *Journal of Materials Chemistry B*, 2015, **3**, 1779-1787.
26. E. A. Rainbolt, K. E. Washington, M. C. Biewer and M. C. Stefan, *Journal of Materials Chemistry B*, 2013, **1**, 6532-6537.
27. J. M. Ren, T. G. McKenzie, Q. Fu, E. H. H. Wong, J. Xu, Z. An, S. Shanmugam, T. P. Davis, C. Boyer and G. G. Qiao, *Chemical Reviews*, 2016, **116**, 6743-6836.
28. W. Wu, W. Wang and J. Li, *Progress in Polymer Science*, 2015, **46**, 55-85.
29. G. Basu Ray, I. Chakraborty and S. P. Moulik, *Journal of Colloid and Interface Science*, 2006, **294**, 248-254.
30. J. K. Kim, S. Y. Yang, Y. Lee and Y. Kim, *Progress in Polymer Science*, 2010, **35**, 1325-1349.
31. K. E. Washington, R. N. Kularatne, J. Du, M. J. Gillings, J. C. Webb, N. C. Doan, M. C. Biewer and M. C. Stefan, *Journal of Polymer Science Part A: Polymer Chemistry*, 2016, **54**, 3601-3608.
32. J. Burke, R. Donno, R. d'Arcy, S. Cartmell and N. Tirelli, *Biomacromolecules*, 2017, **18**, 728-739.

View Article Online
DOI: 10.1039/C7TB01291H

Fully biodegradable amphiphilic thermoresponsive star block copolymers featuring 4 and 6 arms are reported for micellar delivery of doxorubicin.